Diabetes Increases Formation of Advanced Glycation End Products on Sarco(endo)plasmic Reticulum Ca^{2+}-ATPase

Keshore R. Bidasee,[1] Yinong Zhang,[2] Chun Hong Shao,[1] Mu Wang,[2] Kaushik P. Patel,[3] Ü. Deniz Dincer,[4] and Henry R. Besch, Jr.[5]

Prolongation of relaxation is a hallmark of diabetic cardiomyopathy. Most studies attribute this defect to decreases in sarco(endo)plasmic reticulum Ca^{2+}-ATPase (SERCA2a) expression and SERCA2a-to-phospholamban (PLB) ratio. Since its turnover rate is slow, SERCA2a is susceptible to posttranslational modifications during diabetes. These modifications could in turn compromise conformational rearrangements needed to translocate calcium ions, also leading to a decrease in SERCA2a activity. In the present study one such modification was investigated, namely advanced glycation end products (AGEs). Hearts from 8-week streptozotocin-induced diabetic (8D) rats showed typical slowing in relaxation, confirming cardiomyopathy. Hearts from 8D animals also expressed lower levels of SERCA2a protein and higher levels of PLB. Analysis of matrix-assisted laser desorption/ionization time-of-flight mass data files from trypsin-digested SERCA2a revealed several cytosolic SERCA2a peptides from 8D modified by single noncrosslinking AGEs. Crosslinked AGEs were also found. Lysine residues within actuator and phosphorylation domains were cross-linked to arginine residues within the nucleotide binding domain via pentosidine AGEs. Two weeks of insulin-treatment initiated after 6 weeks of diabetes attenuated these changes. These data demonstrate for the first time that AGEs are formed on SERCA2a during diabetes, suggesting a novel mechanism by which cardiac relaxation can be slowed during diabetes. *Diabetes* 53:463–473, 2004

From the [1]Department of Pharmacology, University of Nebraska Medical Center, Omaha, Nebraska; the [2]Department of Biochemistry and Molecular Biology, Indiana University School of Medicine, Indianapolis, Indiana; the [3]Department of Physiology and Biophysics, University of Nebraska Medical Center, Omaha, Nebraska; the [4]Faculty of Pharmacy, University of Ankara, Tandogan, Ankara, Turkey; and the [5]Department of Pharmacology and Center for Vascular Biology and Medicine, Indiana University School of Medicine, Indianapolis, Indiana.

Address correspondence and reprint requests to Keshore R. Bidasee, PhD, 986260 Nebraska Medical Center, Omaha, NE 68198-6260. E-mail: kbidasee@unmc.edu.

Received for publication 13 July 2003 and accepted in revised form 5 November 2003.

6D-2I, 6-week streptozotocin-induced diabetic/2-week insulin treated; 8C, 8-week age-matched control; 8D, 8-week streptozotocin-induced diabetic; AGE, advanced glycation end product; AFGP, 1-alkyl-2-formyl-3,4-glycosyl pyrrole molecule; MALDI-TOF, matrix-assisted laser desorption/ionization time-of-flight; PLB, phospholamban; SERCA2a, sarco(endo)plasmic reticulum Ca^{2+}-ATPase; STZ, streptozotocin.

Reductions in rate and force of cardiac contractions are root causes for the increased incidence of morbidity and mortality among diabetic patients (1–3). Studies show that this "diabetic cardiomyopathy" is independent of coronary vascular diseases and is brought about by shifts in metabolism, cellular biochemistry, and structure (4–8). At the molecular level, decreases in chronotropy and inotropy result from alterations in expression and/or function of several sarcolemmal membrane receptors and associated signal transduction proteins as well as other key proteins involved in regulating/maintaining intracellular ionic homeostasis (9–11). Of particular interest is a transport protein on the sarcoplasmic reticular membrane that plays an integral role in cardiac relaxation. This protein, referred to as sarco(endo)plasmic reticulum Ca^{2+}-ATPase (SERCA2a), is responsible for replenishing intracellular calcium stores following release and in so doing terminate contraction.

SERCA2a is a member of a large family of P-type ATPase enzymes that utilizes the energy generated from hydrolysis of terminal phosphate bond of ATP to pump calcium against its electrochemical gradient (12,13). SERCA1a is the best studied of these single polypeptides. It consists of 10 transmembrane helixes (M1 through M10) and three cytoplasmic domains, referred to as A (actuator), N (nucleotide binding) and P (phosphorylation) domains (14). Translocation of calcium ions from the cytosol to the lumen of the sarcoplasmic reticulum occurs in multiple steps according to the E1-E2 model (15,16). In the first step, calcium ions bind to two high-affinity sites on the cytosolic side. Binding of calcium causes separation of the N, P, and A domains (17–19). The open conformation allows the γ-phosphate of ATP to reach in and phosphorylate aspartate 351 within the P domain ($E1PCa_2$). Phosphorylation of this aspartate residue causes further structural rearrangement of the A, N, and P domains, leading to a state in which the calcium binding sites become low affinity and are exposed to the lumen of the sarcoplasmic reticulum (E2P). Following the loss of calcium, the ATPase becomes dephosphorylated (E2) and is recycled to E1.

Before calcium binding sites become available on SERCA2a, the inhibitory protein phospholamban (PLB) must first dissociate from it. When in the dephosphory-

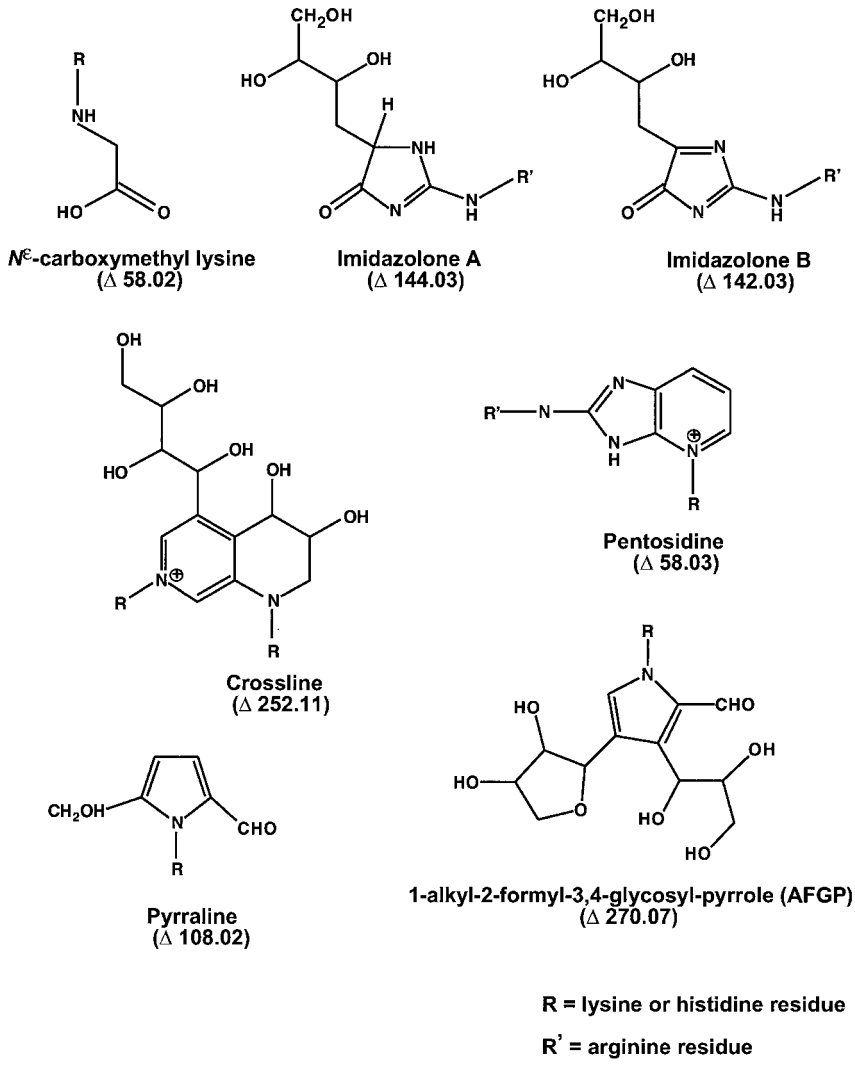

FIG. 1. Structures and Δ-masses of select noncrosslinking and crosslinking AGE molecules investigated in the present study. Configurations were drawn using the algorithm of the software packages of CS Chem 3D Pro version 5 (Cambridge Scientific Computing, Cambridge, MA).

lated state, PLB interacts with SERCA2a at two sites: one on the cytoplasmic side (with sequence KDDKPV) and the other within the transmembrane helixes, possibly in the groove formed between transmembrane segments M2, M4, M6, and M9 (20–22). When serine-16 and/or threonine-17 become phosphorlyated PLB detaches from SERCA2a. This detachment exposes the high-affinity calcium binding sites.

Most studies attribute the slowing in cardiac relaxation developed during diabetes principally to *1*) a decrease in expression of SERCA2a, *2*) an increase in expression of PLB, or *3*) a decrease in SERCA2a-to-PLB ratio (23–32). Recently, Trost et al. (33) and Vetter et al. (34) provided strong evidence supporting this notion when they showed that overexpression of SERCA2a improves loss in cardiac contractility induced by diabetes. However, there are studies suggesting that a decrease in expression of SERCA2a or an increase in PLB may not fully account for diabetes-induced slowing in cardiac relaxation. As examples, Russ et al. (35) and Zarain-Herzberg et al. (36) found no significant loss in SERCA2a expression in hearts with established diabetic cardiomyopathy. Recently, Ye et al. (37) showed that overexpression of the antioxidant protein metallothionein reversed the slowing in intracellular Ca^{2+} decay induced by diabetes. Candido et al. (38) also found that treatment with a breaker of advanced glycation end products (AGEs) prevents diabetes-induced structural changes to the myocardium. The latter two studies suggest that in addition to changes in expression, a long-lived protein like SERCA2a ($t_{1/2}$ ~14 days) (39) may become posttranslationally modified during diabetes. These modifications, especially the types that crosslink SERCA2a domains, could disrupt the tightly regulated process involved in translocation of calcium ions.

The present study was designed to investigate whether one type of modification, namely AGEs, increases on SERCA2a during diabetes and if production of these complexes could be attenuated with insulin treatment.

RESEARCH DESIGN AND METHODS

Mouse monoclonal SERCA2a and phospholamban antibodies were obtained from Affinity Bioreagents (Golden, CO). Actin antibodies (C-11) were purchased from Santa Cruz Biotechnology (Santa Cruz, CA). Brevital (methohexital sodium) and NPH Ilentin II (intermediate-acting insulin) were obtained from Eli Lilly (Indianapolis, IN). Other reagents and solvents used were of analytical grade.

Induction and verification of experimental streptozotocin-induced diabetes. All animal procedures were carried out in accordance with guidelines established by institutional animal care and use committees and are described in detail elsewhere (40–42). Briefly, male Sprague-Dawley rats weighing between 180–190 g were anesthetized with Brevital (25 mg/kg i.p.) or isofluorane and then injected via tail vein with either streptozotocin (STZ) in

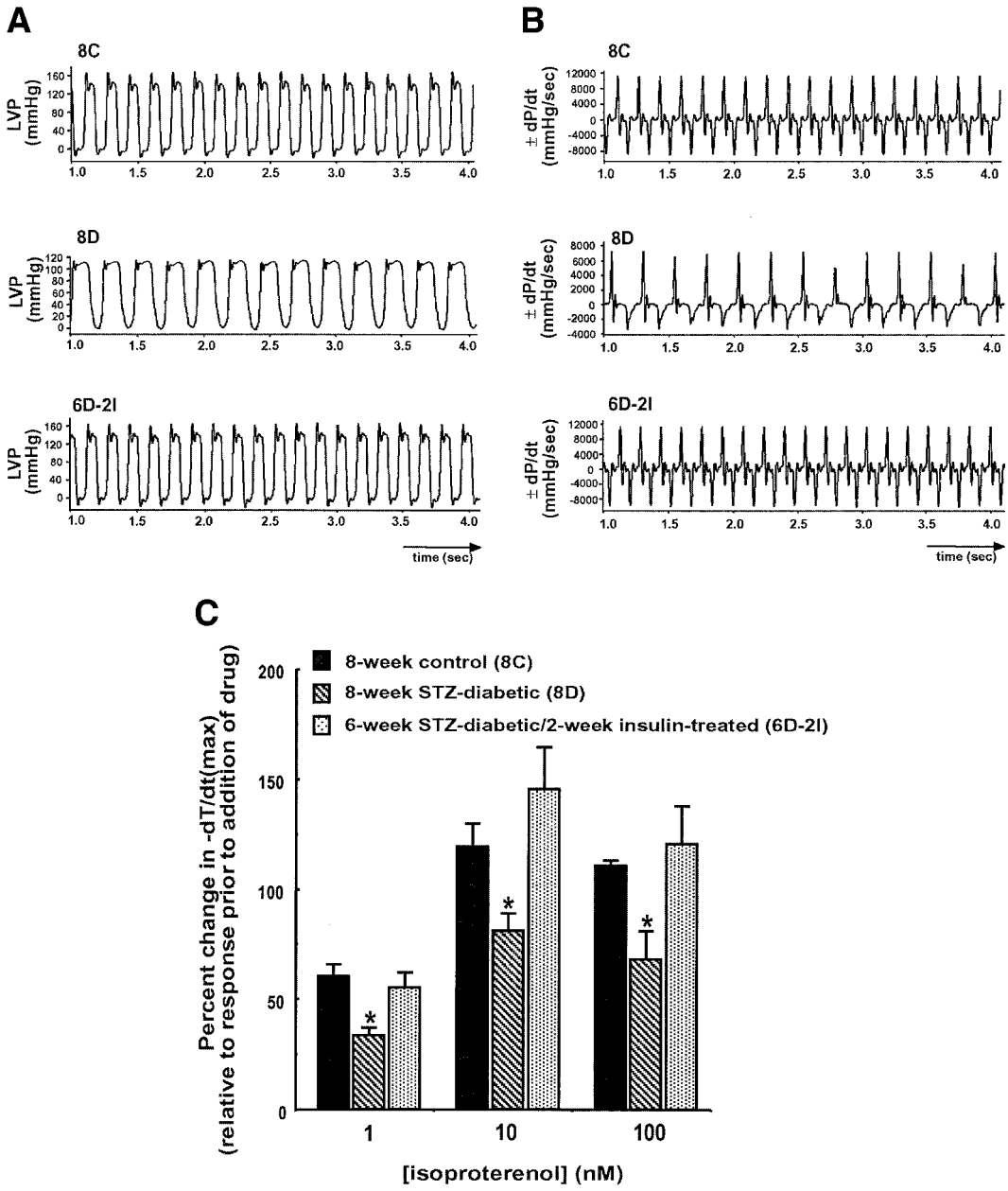

FIG. 2. Representative 3-s recordings of direct in vivo left ventricular measurements from 8C, 8D, and 6D-2I rats (*A*) as well as the rate derivatives ± dP/dt (*B*). For this, animals were lightly anesthetized with Inactin (20 mg/kg) and a pressure transducer attached to the end of a catheter was inserted into the left ventricle by way of the carotid artery. Note that diabetes decreases heart rate and left ventricular pressure, slows the rate of relaxation, and increases left ventricular end diastolic pressure, consistent with diabetic cardiomyopathy. *C*: Comparison of rate of relaxation (−dT/dt) at peak of hearts from 8C, 8D, and 6D-2I animals following isoproterenol stimulation. For this, hearts were excised, cannulated via aorta, and perfused retrograde with Krebs-Henseleit buffer at 37°C. The apex of ventricle was treaded and connected to force displacement transducer. The right atrium was then removed, the arteriovenous node was crushed, and pacing of the heart was kept constant (190–200 bpm) by external stimulation. Bolus doses (1, 10, and 100 nmol/l) of isoproterenol were then perfused, and changes in isometric developed tension and its rate derivative −dT/dt (at maximum) were determined. Data are means ± SE for three experiments. *Denotes value significantly different from 8C and 6D-2I rats.

0.1 mol/l citrate buffer, pH 4.5 (50 mg/kg), or citrate buffer. Three days later, blood glucose levels were determined using a Glucometer II and Glucostix (Peridochrom Glucose GOD-PAP Assay Kit; Roche Molecular Biochemicals, Indianapolis, IN). Throughout this study, animals were housed in pairs (similar weights to minimize dominance) at 22°C with fixed 12-h light/dark cycles and given free access to food and water.

Insulin treatment protocol. Six weeks after the STZ injection, diabetic animals were randomly divided into two subgroups. One subgroup was placed on an insulin regimen (NPH Ilentin II; Lilly, Indianapolis, IN) for 2 weeks. Tail blood glucose levels of these animals were measured daily (between 9:00 and 10:00 A.M.), and insulin doses were individually adjusted so as to maintain euglycemic states. The other subgroup of diabetic animals continued as nontreated diabetic subjects for 2 additional weeks. Any diabetic animal whose body weight fell by >10% of initial starting body weight during in vivo protocol was killed and eliminated from the study.

Sample collection. Animals were given a single lethal dose of Brevital (75 mg/kg i.p.) or Inactin (thiobutabarbital, sodium salt, 60 mg/kg i.p). Abdominal cavities were opened and blood samples were collected from left renal arteries (43). HbA_{1c} levels were determined from whole blood using Roche Diagnostics Unimate 5 assay kit (Roche Diagnostics, Indianapolis, IN), and insulin was assayed from serum using Mercoda rat insulin ELISA kit (Alpco Diagnostics, Salem, NH). After removal of blood, chest cavities were opened and hearts from 8-week age-matched control (8C), 8-week STZ-induced diabetic (8D), and 6-week STZ-induced diabetic/2-week insulin-treated (6D-2I) animals were excised. Hearts assigned for measurement of cardiac function

TABLE 1
Hemodynamics parameters of 8C, 8D, and 6D-2I animals

Hemodynamic parameters	8C	8D	6D-2I
n	9	8	8
Heart rate (bpm)	338.6 ± 8.5	268.1 ± 18.6*	347.4 ± 12.6
Left ventricular pressure (mmHg)	133.0 ± 3.3	104.7 ± 14.3*	134.0 ± 2.7
Left ventricular end diastolic pressure (mmHg)	−3.94 ± 0.5	5.78 ± 3.8*	−2.8 ± 1.7
$-dP/dt_{max}$ (mmHg/s)	−8,065.5 ± 995.4	−5,279.6 ± 1,096.6*	−8,203.8 ± 723.9

Data are means ± SE. *Values significantly different from controls at $P < 0.05$.

using modified Langendorff procedure were immediately placed in oxygenated Kreb-Henseleit buffer (118 mmol/l NaCl, 27.2 mmol/l $NaHCO_3$, 4.8 mmol/l KCl, 1.2 mmol/l $MgSO_4$, 1.0 mmol/l KH_2PO_4, 1.25 mmol/l $CaCl_2$, and 11.0 mmol/l glucose at 37°C), and those to be used for measurement of SERCA2a and PLB content were quick-frozen by embedding in crushed dry ice.

Measurement of cardiac function. Two procedures were used to compare cardiac function among animals from the three experimental groups. In the first procedure, in vivo left ventricular function (±dP/dt, left ventricular end diastolic pressure, and heart rate) was evaluated in anesthetized animals (at least four animals per group) to ascertain changes in basal cardiac function induced by diabetes. For this, animals were lightly anesthetized with Inactin (20 mg/kg i.p), and a catheter containing a pressure transducer was inserted via the carotid artery into the left ventricle to determine basal heart rate, left ventricular pressure, left ventricular end diastolic pressure, and the derivatives ± dP/dT, as previously described (44). Powerlab data acquisition system (ADInstruments, Colorado Springs, CO) was used for acquiring and analyzing measurements. In the second procedure, isoproterenol-induced contraction/relaxation properties of hearts from 8C, 8D, and 6D-2I animals were compared using a modified isobaric Langendorff procedure (45) under similar perfusion conditions. For this, hearts were excised from animals, cannulated via the aorta, and then perfused retrograde at a flow rate of 10 ml/min with oxygenated standard Krebs-Henseleit buffer (37°C). The right atrium was then removed and the ventricle was pierced at the apex and connected to a force displacement transducer (FT03C; Grass Instrument, Quincy, MA) via silk thread for measurement of developed tension. Arteriovenous node was crushed and the ventricle was then stimulated at a constant pacing rate of 190–200 bpm. After establishing basal isometric tension, hearts were then challenged with freshly prepared isoproterenol bitartrate (1, 10, and 100 nmol/l, given as bolus via a side arm in aortic cannula) and changes in isometric developed tension (at peak) were determined. Changes in relaxation rates ($-dT/dt_{max}$) were determined and used in this study as indirect indexes of SERCA2a activity. Hearts used for evaluation of cardiac function employing the Langendorff procedure were not used for biochemical analyses.

Relative levels of SERCA2a mRNA in 8C, 8D, and 6D-2I rat hearts. Total RNA was extracted separately but simultaneously from 8C, 8D, and 6D-2I rat hearts using Quick Prep total RNA extraction kits (Amersham Pharmacia Biotech, Piscataway, NJ) as previously described (40–42). Thereafter, equivalent amounts of RNA from each of 8C, 8D, and 6D-2I (with distinct 18S and 28S bands on formamide agarose gels, three separate preparations) were used to synthesize 1st strand cDNA. PCRs were then carried out using the following program: 5 min denaturation (94°C), 1 min annealing (56.7°C), 2 min extension (72°C), repeated for a total of 37 cycles. Primers for SERCA2a were sense (5′-GAAGATGAATGATTCGACACG-3′) and antisense (5′-TGGAGAAGTTGT CGTCGG-3′), whereas those for β-actin were sense (5′-CGTAAAGACCTCTA TGCCA-3′) and antisense (5′-AGCCATGCCAAATGTCTCAT-3′).

Relative levels of SERCA2a and phospholmban proteins in 8C, 8D, and 6D-2I rat hearts. Relative levels of SERCA2a and phospholamban proteins were determined in two steps. First, membrane vesicles were prepared simultaneously from hearts of 8C, 8D, and 6D-2I animals (two hearts per preparation × 3 preparations) using procedures previously described (40–41). Second, 60 μg of total protein from each preparation was solubilized in gel dissociation medium containing 10 mg/ml dithiothreitol and then loaded onto denaturing 4–20% linear gradient polyacrylamide gels. Only those samples used for analysis of SERCA2a were boiled for 15 min before loading onto the gels. The gels were then electrophoresed at 150V at 4°C for 3.5 h for SERCA2a or 1.5 h for PLB. Proteins on the gels were then transferred for 1 h at 400 mA onto polyvinylidene difluoride membrane using a semi-dry procedure, as previously described. The membrane was then probed for SERCA2, PLB, and β-actin proteins, as previously described (40–42).

Identification and localization of glycation end products on SERCA2a from 8C, 8D, and 6D-2I rat hearts. AGEs were identified using the procedures previously described (42,46,47). In this study, we investigated N^{ε}-(carboxymethyl)-lysine, imidazolone A, imidazone B, pyrraline, and 1-alkyl-2-formyl-3,4-glycosyl pyrrole molecule (AFGP) as well as crosslinking AGEs crossline and pentosidine (Fig. 1). Two restriction criteria were employed when searching for noncrosslinking AGEs: *1*) only a single modification was

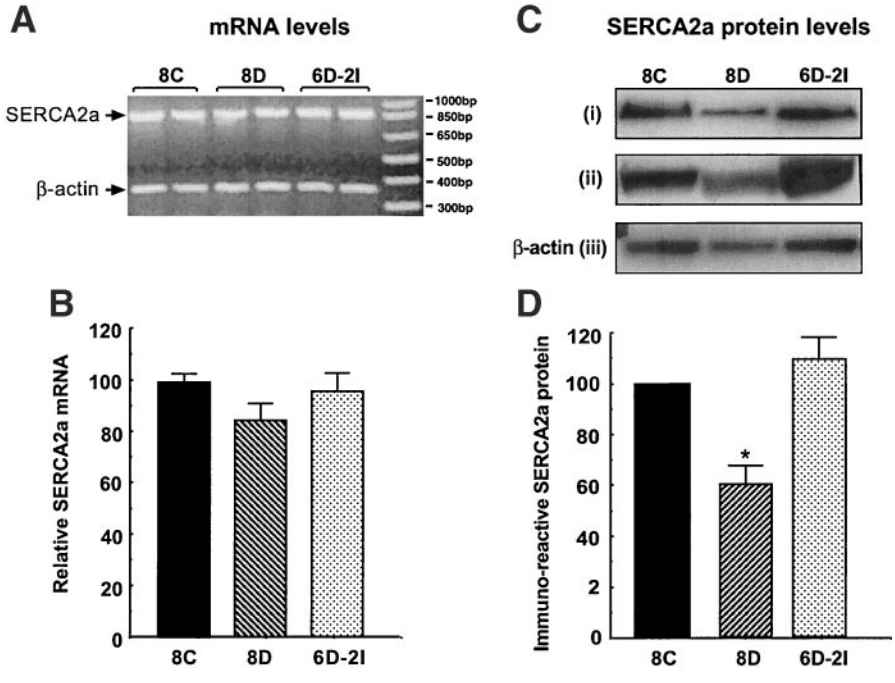

FIG. 3. SERCA2a expression in hearts from 8C, 8D, and 6D-2I animals. *A* and *B*: Total RNA was reverse-transcribed into 1st cDNA using oligo dT_{15} and Superscript II. Primers were then used in PCR to simultaneously amplify segments of cDNA encoding SERCA2a and β-actin. *A*: Representative electrophoretogram showing SERCA2a (872 bp) and β-actin (387 bp). *B*: Signal intensities normalized to concomitant β-actin (means ± SE obtained from three hearts analyzed in duplicate). *C*: Amount of SERCA2a protein in 60 μg of membrane vesicles. Upper panels show representative Western blot for SERCA2a from three membrane preparations. Note shift in the electrophoretic mobility in 8D (*D*). Graph shows means ± SE (normalized to concomitant β-actin) from three experiments done in duplicate using three membrane preparations. *Denotes values significantly different from 8C and 6D-2I.

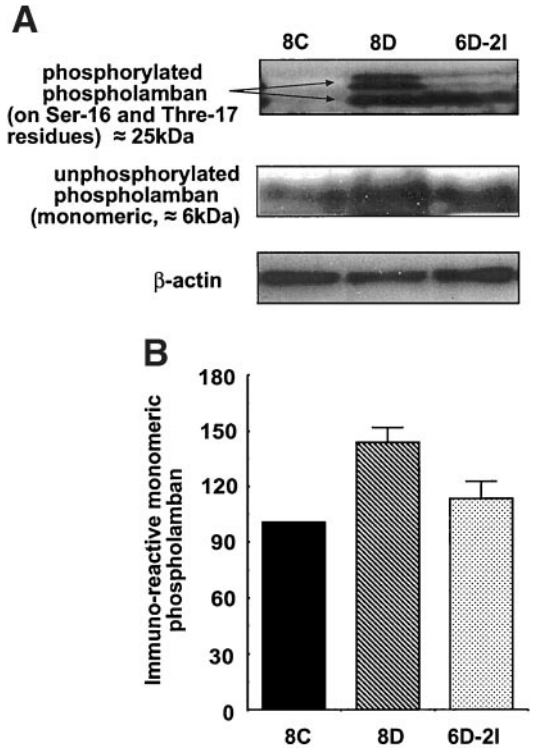

FIG. 4. Relative levels of PLB protein in hearts from 8C, 8D, and 6D-2I animals. Hearts phosphorylated (*top panel*) and unphosphorylated (*middle panel*) in 100 μg of membrane vesicles from 8C, 8D and 6D-2I animals. A typical autoradiogram from Western blot analysis for internal reference, β-actin is shown (*bottom panel*). Graph shows means ± SE for three experiments done in duplicate using three membrane preparations.

allowed within the peptide fragment and *2*) the peptide must contain one missed cleavage at a lysine or arginine residue (or no miscleavage but containing a histidine residue). For crossline, the crosslinkage must occur between lysine residues on the two peptides, and for pentosidine AGEs the crosslinkage must occur between a lysine residue on one peptide and an arginine residue on the other.

Data analysis and statistics. Differences between values from each of the 8C, 8D, and 6D-2I rats were evaluated using the nonparametric Kruskal-Wallis (GBStat version 6.5.4; Dymanic Microsystems, Silver Spring, MD). The data shown are means ± SE and results are considered significantly different if $P < 0.05$.

RESULTS

Mean body weight of animals at the start of study was 187.2 ± 2.0 g. After 56 days, weight of 8C animals increased to 399.0 ± 8.7 g ($n = 12$), whereas those of 8D animals increased to 225.4 ± 10.4 g ($n = 13$, $P < 0.05$). Although diabetic animals did not gain weight as rapidly, they fed normally and moved around in their cages freely. Two weeks of insulin treatment initiated after 6 weeks diabetes duration restored loss in body weight (279.6 ± 13.1 g, $n = 12$). Initial average glucose level was 4.4 ± 0.1 mmol/l. Mean blood glucose level of 8C animals remained low (3.9 ± 0.3 mmol/l). Three days after injection with STZ, mean blood glucose levels of diabetic animals were 20.7 ± 0.6 mmol/l. This level increased progressively to a high of 28.5 ± 2.5 mmol/l on day 56. Insulin treatment also lowered mean blood glucose level to 5.1 ± 3.8 mmol/l. Serum insulin levels were significantly lower in 8D animals (0.5 ± 0.1 ng/ml compared with 2.6 ± 0.5 ng/ml in 8C animals). Heart–to–body weight ratios were significantly higher in 8D compared with 8C animals (4.13 ± 0.2 mg/g vs. 3.0 ± 0.1 mg/g). This ratio returned to nearly 8C values with insulin treatment (3.76 ± 0.2 mg/g). HbA_{1c} levels in 8C, 8D, and 6D-2I animals were 4.3 ± 0.1, 9.5 ± 0.25, and 5.8 ± 0.5%, respectively.

Confirming diabetic cardiomyopathy. Before conducting biochemical analyses, left ventricular function (in vivo and in vitro) of hearts from 8C, 8D, and 6D-2I animals were evaluated to establish cardiomyopathy. Consistent with other studies, data from both techniques used in this study confirm that diabetes decreases rate of cardiac relaxation in rat hearts.

By inserting a pressure transducer into the left ventricle of lightly anesthetized rats, we found that after 8 weeks of diabetes basal heart rate, left ventricular pressure, and its derivative $-dP/dt_{max}$ decreases whereas left ventricular end diastolic pressure increases. These changes can be seen clearly (Fig. 2*A* and *B*) and show representative 3-s tracings of basal hemodynamics from 8C, 8D, and 6D-2I animals. Most obvious (Fig. 2*A*) are the decreases in heart rate and the slowing in decrease in left ventricular pressure decay. The latter is shown more clearly (Fig. 2*B* [*8D panel*]). On closer examination, it is also very clear that left ventricular end diastolic pressure increases in the diabetic heart, possibly reflecting ventricular stiffness. Two weeks of insulin treatment initiated after 6 weeks of diabetes prevented and/or minimized the slowing in heart rate, the decrease in left ventricular pressure (and its derivatives ± dP/dt), and the increase in left ventricular end diastolic pressure. A summary of hemodynamic changes induced by 8 weeks of diabetes and its reversal with insulin treatment is shown in Table 1.

When paced at 190 bpm in a Langendorff apparatus, hearts from 8D animals developed significantly less tension compared with 8C animals (7.0 ± 0.5 g tension compared with 9.5 ± 1.2 g), consistent with cardiomyopathic hearts. Two weeks of insulin treatment initiated after 6 weeks of diabetes minimally improve basal developed tension (7.2 ± 0.6 g). When hearts from 8C animals were challenged with bolus 1 nmol/l isoproterenol, developed tension increased to 18.1 ± 1.2% over basal within 12 s. This increase persisted for ~3 s and then gradually subsided. Further increases in developed tension were also obtained when 8C hearts were stimulated with 10 nmol/l and 100 nmol/l isoproterenol (amplitude of the increases were 28.6 ± 2.5 and 24.7 ± 1.3% over basal, respectively). On the other hand, when hearts from 8D animals were stimulated with 1 nmol/l isoproterenol, minimal changes in isometric developed tension were observed. On stimulation with 10 nmol/l isoproterenol, the peak response took almost 35 s to be attained, but developed tension increased by 80.3 ± 5.6%. Interestingly, the peak response also persisted for >2 min and subsided to basal levels 5 min after addition of the drug. Increasing the concentration of isoproterenol to 100 nmol/l resulted in a 70 ± 8.7% increase in developed tension. These data are consistent with the lower sensitivity of diabetic hearts to isoproterenol. When hearts from 6D-2I animals were challenged with 1, 10, and 100 nmol/l isoproterenol, developed tension increased by 20.2 ± 6.5, 35.1 ± 5.4, and 33.2 ± 5.3% over basal, and the time to peak response was of the order of 12–15 s (similar to those of control animals). Responses of hearts from 6D-2I animals also

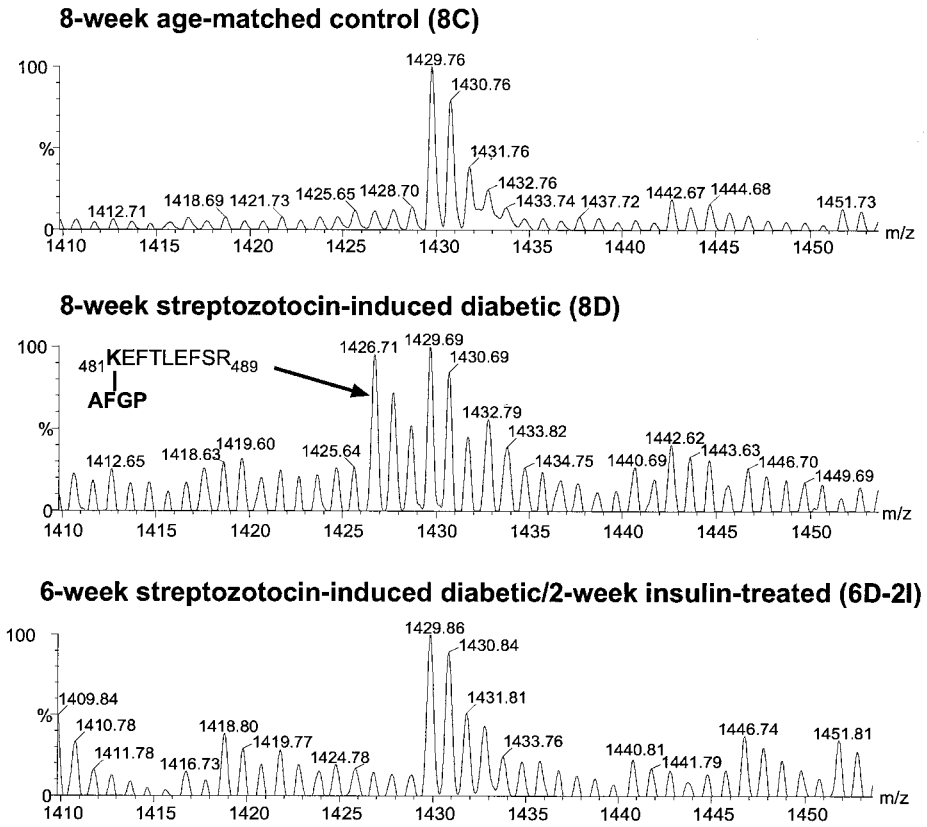

FIG. 5. Alignment of a select region of MALDI-TOF mass spectra obtained from trypsin digestion of SERCA2a from 8C, 8D, and 6D-2I animals. Spectra in the 8D panel show the prominence of monoisotopic peak at 1426.71 Da. This signal is not present in spectra from 8C or 6D-2I. This peak is likely to result from an AFGP modification on lysine 481 present on the miscleaved peptide $_{481}$KEFTLEFSR$_{489}$. Bold lettering indicates the amino acid that is modified.

persisted for >90 s. Thus, insulin treatment is able to restore diabetes-induced loss in isoproterenol sensitivity.

Figure 2*C* shows the summary of the changes in $-dT/dt_{max}$ when hearts from 8C, 8D, and 6D-2I animals were challenged with 1, 10, and 100 nmol/l isoproterenol. These data are in agreement with those of Dincer et al. (48) and Afzal et al. (49) and clearly show that diabetes decreases relaxation rates. Taken together, data from in vivo ventricular function measurements and isobaric Langendorff procedure establish that after 8 weeks of diabetes left ventricular function was compromised and that 2 weeks of insulin treatment initiated after 6 weeks of diabetes prevented and/or reversed this dysfunction.

Relative levels of mRNA encoding SERCA2 from 8C, 8D, and 6D-2I rat hearts. After normalizing to concomitant β-actin, mRNA encoding SERCA2a decreased by 15.6 ± 8.3% following 8 weeks of STZ-induced diabetes (Fig. 3*A*). However, this difference was not significant from age-matched controls ($P > 0.05$). Steady-state levels of mRNA encoding SERCA2a in hearts from 6D-2I animals were similar to that of 8C animals (96.9 ± 7.1% of control). Nucleotide sequence analyses and restriction mapping confirmed that the PCR products generated in the PCRs were derived from specific amplification of mRNA encoding SERCA2a (data not shown).

Relative levels of SERCA2 protein in hearts from 8C, 8D, and 6D-2I rats. After normalization to concomitant β-actin protein, immunoreactive SERCA2a protein from 8D rat hearts was 39.9 ± 7.2% lower than age-matched 8C rats (Fig. 3*B*) ($P < 0.05$). On some Western blots it is apparent that diabetes may be altering the electrophoretic mobility (SDS-PAGE) of SERCA2a. In one preparation (made from two hearts), the electrophoretic mobility of SERCA2a from 8D was faster than that of 8C and 6D-2I (see Fig. 2*B* [middle panel]), whereas in another preparation the electrophoretic mobility of SERCA2a from 8D was slower. The shift in electrophoretic mobility is likely due to posttranslation modifications. Two weeks of insulin-treatment, initiated after 6 weeks of diabetes minimized and/or prevented loss in SERCA2 expression (109.2 ± 2.2% of control).

Relative levels of PLB protein in hearts from 8C, 8D, and 6D-2I rats. After 8 weeks of STZ-induced diabetes, steady-state levels of immunoreactive monomeric (dephosphorylated) PLB increased significantly in hearts from 8D rats (Fig. 4*A*). When normalized to concomitant β-actin protein, the magnitude of the increase was 40 ± 4.2% over control. Two weeks of insulin-treatment initiated after 6 weeks of diabetes prevented (and/or reversed) the increase in expression induced by diabetes. In this study, steady-state levels of phosphorylated pentameric PLB also increased with diabetes. Two distinct phosphorylated forms of PLB proteins were detected, likely suggesting mono- (either on serine-16 or threonine-17) and diphosphorylation (both serine-16 and threonine-17). Two weeks of insulin treatment decreased steady-state levels of immunoreactive diphosphorylated PLB (assuming that the higher running of the two bands reflect the diphosphor-

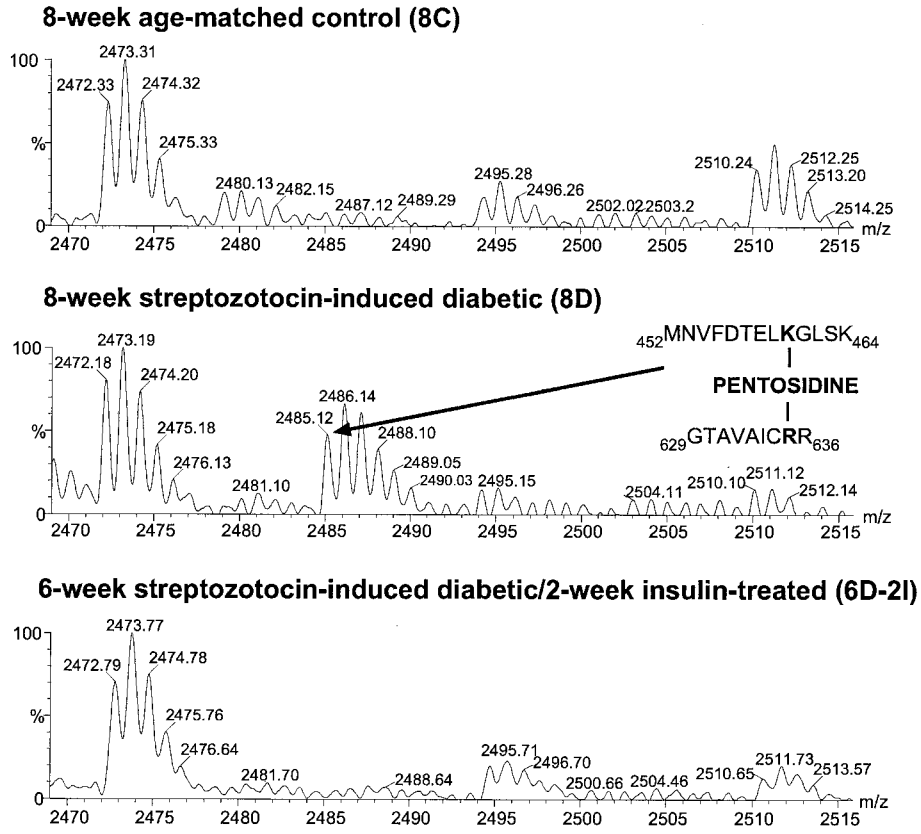

FIG. 6. Alignment of a select region of MALDI-TOF mass spectra obtained from trypsin digestion of SERCA2a from 8C, 8D, and 6D-2I animals. Spectra in the 8D panel show the prominence of monoisotopic peak at 2,485.12 Da. This signal is not present in spectra from 8C or 6D-2I. This peak is likely to result from crosslinking of lysine 460 on the miscleaved peptide $_{452}$MNVFDTELKGLSK$_{464}$ and arginine 635 on the miscleaved peptide $_{629}$GTAVAICRR$_{636}$ via pentosidine. Bold lettering indicates the amino acid that is modified.

ylated form). Insulin treatment did not change the amount of monophosphorylated PLB induced by diabetes.

Trypsin digestion of SERCA2a from 8C, 8D, and 6D-2I rat hearts and determination of peptide masses. Overnight digestion of SERCA2a from 8C with trypsin afforded 75 peptides with monoisotopic between 700 and 2,500 Da. Of these, 26 (35%) correspond to theoretical trypsin fragments (nonmodified) generated in silico from rat SERCA2a (GenBank accession no. B31982), spanning the entire range of the rat SERCA2a protein with minimum variability (≤560 ppm). Digestion of SERCA2a from 8D animals with trypsin afforded 60 peptides, 14 (23%) of which represented nonmiscleaved/nonmodified theoretical SERCA2a peptides. Only seven of these peptides were a subset of 8C peptides, suggesting that diabetes is inducing changes to SERCA2a that compromise trypsin's ability to digest it. Trypsin digestion of SERCA2a from 6D-2I animals afforded 50 peptides with monoisotopic ranging from 700 to 2,500 Da. Of these, 22 (44%) corresponded to the masses of nonmodified trypsin-derived peptides from rat SERCA2a, and 16 of them were identical to 8C peptides. Thus, insulin treatment only partially attenuated trypsin-sensitive formation of post-translational modifications on SERCA2a (modifications at lysine and arginine residues).

Identification of glycation products on SERCA2a. The next step was to search the matrix-assisted laser desorption/ionization time-of-flight (MALDI-TOF) mass data files to determine whether AGEs are formed on SERCA2a, and if so, what type of AGEs are formed and where they are located on protein. In the first step of the protocol, rat SERCA2a (GenBank accession no. B31982) was digested in silico and $M+H^+$ of all possible peptides (including cysteine with iodoacetamide and acrylamide adducts, oxidized methionines, and one miscleavage) were uploaded into the PERL algorithm along with the MALDI-TOF mass data files. The data files were then searched for select noncrosslinking N^{ϵ}-(carboxymethyl)-lysine, imidazolone A, imidazone B, pyrraline, and AFGP as well as crosslinking AGEs (crossline and pentosidine). During the analyses, $M+H^+$s that were found in the mass files of all three 8C, 8D, and 6D-2I samples and not attributed to SERCA2a peptides were considered contaminants and eliminated.

As an example, search of data files revealed a monoisotopic mass of 1426.71 Da that is prominent in 8D but not in 8C and 6D-2I samples (Fig. 5). Since no peptide generated from trypsin-digestion of SERCA2a possesses an $M+H^+$ of 1,426.71 ± 0.5 Da, this $M+H^+$ likely reflects the mass of a SERCA2a peptide from 8D samples that contains an AGE adduct. The next step was to determine the nature of the modification and which peptide fragment (amino acid) contained this adduct. For this, the algorithm searched the theoretical SERCA2a digestion file for $M+H^+$s that were 58.02, 58.03, 108.02, 142.03, 144.03, 252.11, or 270.07 Da < 1,426.71 ± 0.5 Da. No $M+H^+$ of 1,368.69 (i.e., 1,426.71–58.02), 1,318.69, 1,284.68, 1,282.68, 1,368.68, or 1,174.60 Da, respectively, were detected in the theoretical mass file, suggesting that these masses do not correspond to

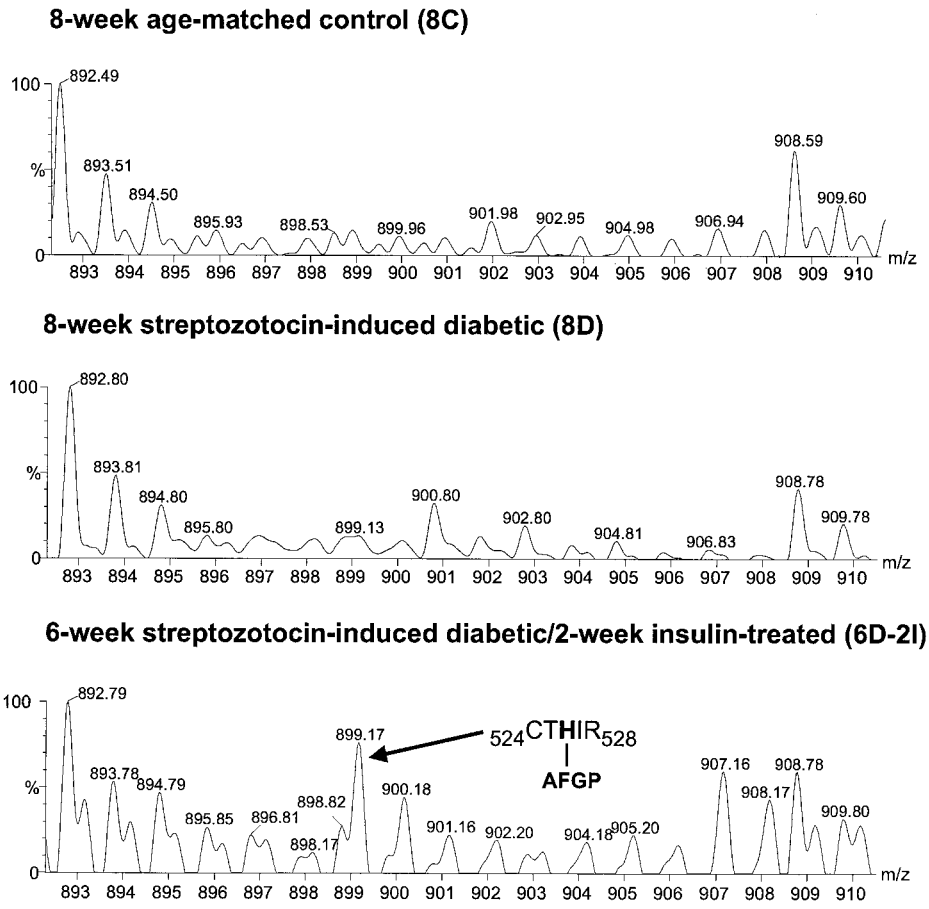

FIG. 7. Alignment of a select region of MALDI-TOF mass spectra obtained from trypsin digestion of SERCA2a from 8C, 8D, and 6D-2I animals. Spectra in the 6D-2I panel show the prominence of monoisotopic peak at 899.17 Da. This signal is not present in spectra from 8C or 8D. This peak is likely to result from an AFGP modification on histidine 526 present on the miscleaved peptide $_{524}$CTHIR$_{528}$. Bold lettering indicates the amino acid that is modified.

masses of trypsin-derived SERCA2a peptides. However, an $M+H^+$ of 1,156.60 ± 0.1 Da was detected. This $M+H^+$ corresponds to the mass of the miscleaved peptides $_{481}$**K**EFTLEFSR$_{489}$. The subscript numbers represent the location of these peptides on rat SERCA2a and the bold letter indicates the miscleaved site. Therefore, an $M+H^+$ of 1,426.71 in 8D samples corresponds to the mass of the peptide $_{481}$**K**EFTLEFSR$_{489}$ modified at arginine 481 with an AFGP adduct. As a second example, search of MALDI-TOF mass files revealed a monoisotopic mass of 2,485.12 Da is prominent in 8D but not in 8C and 6D-2I samples (Fig. 6). Using the PERL algorithm, this $M+H^+$ was identified as the mass of two peptides ($_{452}$MNVFDTEL**K**GSLK$_{464}$ and $_{629}$GTAVAIC**R**R$_{637}$) crosslinked with pentosidine via lysine 460 and arginine 635.

Modifications were not found only on peptides from 8D samples. Some peptides from insulin-treated SERCA2a also contained modifications that were either less prominent or absent altogether from SERCA2a of 8D samples and absent from SERCA2a from 8C samples. An $M+H^+$ of 899.17 Da was detected in mass data file from 6D-2I SERCA2a samples (Fig. 7), but barely seen in diabetic SERCA2a (899.13 Da) and absent from 8C samples. Analysis of this data revealed that this $M+H^+$ is attributed to a single AFGP (+270.07 Da) adduct on the histidine-3 residue within the peptide $_{1}$CT**H**IR$_{7}$ (629.32 Da). It should be pointed out that the $M+H^+$ of 908.60 ± 0.3 Da in all three samples (Fig. 7) could reflect a contaminant because this $M+H^+$ is not the mass of any of the theoretical SERCA2a peptides.

Unlike in previous studies (45–47), we did not detect modifications resulting from N^{ϵ}-(carboxymethyl)-lysine, pyralline and crossline, attesting to the uncertainty as to which AGEs are formed on which protein and under what conditions. We also did not detect the AGEs precursors, Schiff bases, and Amadori products on SERCA2a. A complete listing of AGE modifications detected on SERCA2a is given (Table 2). It should also be mentioned that a few noncrosslinking AGEs were also localized to consensus SERCA2a peptides from 8C, 8D, and 6D-2I samples. These modifications were not included in Table 2 as we felt that they were attributed to the natural aging process and not to the diabetes.

DISCUSSION

The present study shows for the first time that AGEs are formed on intracellular SERCA2a during chronic diabetes. They are also the first to pinpoint the specific amino acids within the SERCA2a sequence where AGEs modifications occur. These posttranslational modifications were detected by digesting SERCA2a with trypsin, determining the masses of peptides using MALDI-TOF mass spectrometry, and then searching the data files for AGEs using an

TABLE 2
Amino acids on SERCA2a modified with AGES during chronic diabetes

Amino acid sequence of peptides detected with AGE modification	Type of AGE modification	Theoretical mass ($M+H^+$) of AGE modified peptide (Da)	Measured mass ($M+H^+$) of AGE modified peptide (Da)	Δ Mass (Da)
$_{524}$CT**H**IR$_{528}$ (diabetic)	Imidazolone A	773.34	773.64	+0.30
$_{524}$CT**H**IR$_{528}$ (insulin treated)	AFGP	899.39	899.17	−0.22
$_{629}$GTAVAIC**R**R$_{637}$ (diabetic)	Imidazolone A	1,090.54	1,090.46	−0.08
$_{159}$VPADI**R**LTSIK$_{169}$ (insulin)	Imidazolone B	1,354.75	1,354.64	−0.11
$_{481}$**K**EFTLEFSR$_{489}$ (diabetic)	AFGP	1,426.67	1,426.71	+0.04
$_{468}$ANACNSVI**K**QLMK$_{480}$ (diabetic)	AFGP	1,689.81	1,689.82	+0.01
$_{140}$I**K**AK$_{143}$ | $_{674}$CFA**R**VEPSHK$_{683}$ (diabetic)	Pentosidine	1,689.94	1,689.82	−0.08
$_{135}$**K**SVQR$_{139}$ | $_{1199}$VPADI**R**LTSIK$_{205}$ (diabetic)	Pentosidine	1,887.13	1,886.87	−0.30
$_{135}$**K**SVQR$_{139}$ | $_{651}$AFTG**R**EFDELSPSAQR$_{666}$ (diabetic)	Pentosidine	2,485.27	2,485.12	−0.15
$_{452}$MNVFDTEL**K**GLSK$_{464}$ | $_{629}$GTAVAIC**R**R$_{637}$ (diabetic)	Pentosidine	2,485.32	2,485.12	−0.20
$_{615}$QAGI**R**VIMITGDNK$_{628}$ | $_{678}$VEPSH**K**SK$_{685}$ (diabetic)	Pentosidine	2,484.35	2,485.12	−0.72

in-house PERL algorithm. Imidazolone A was found on the A domain (on arginine 164), AFGP was found on the P domain (on lysine 481), and imidazolone A, imidazolone B, and AFGP were found on the N domain (on histidine 526 and arginine 635). In addition, a large number of pentosidine crosslinkages were also found intra- and interdomains. One crosslinkage was found within the A domain (between lysine 135 and arginine 204), two between A and N domains (between lysine 142 and arginine 677, and between lysine 135 and arginine 655), one between P and N domains (between lysine 460 and arginine 636), and one within the N domain (between lysine 683 and arginine 619). It should be pointed out that none of these AGEs adducts were found within the transmembrane helixes. The latter is expected because these regions are not in direct contact with the high cytosolic concentrations of reducing aldose and ketose sugars.

These data also suggest a novel mechanism by which rate of cardiac relaxation can be prolonged during diabetes. By disrupting intra- and interdomain tertiary structures, AGEs complexes can compromise structural movements required for translocating calcium ions from the cytosol to the lumen of the sarcoplasmic reticulum, and this could lead to a lowering in the activity of SERCA2a. As an example, since A, P, and N domains were found to be crosslinked with AGEs during diabetes, it is likely that the open structure conformation required for phosphorylation may not be readily achieved, leading to loss in activity.

A second major finding of the present study is that SERCA2a from 6D-2I animals no longer contained crosslinking AGEs and had fewer noncrosslinking AGEs compared with SERCA2a from 8D animals. Why crosslinking but no noncrosslinking AGEs were found remains unclear. Nonetheless, since rates of relaxation were noticeably improved in 6D-2I animals, it is likely that crosslinking AGEs adducts more severely compromise SERCA2a ability to pump calcium ions than do noncrosslinking AGEs.

We also found that although steady-state levels of mRNA encoding SERCA2a were not significantly altered by diabetes, steady-state levels of immunoreactive SERCA2a protein decreased. One simple explanation for unchanged mRNA levels may be that too many cycles were used for PCRs (measurements were made at the plateau phase of the product formed versus cycle number curve). We are in the process of conducting real-time PCR to address this question. Alternatively, since steady-state protein level is the sum product of its rates of transcription, translation, and degradation, it is likely that either translation rates of SERCA2a protein may be slower than transcription rates or degradation rates of SERCA2a protein are faster than transcription and translation rates combined.

We did not detect any immunoreactive phosphorylated PLBs in control samples. This was very surprising because samples for SDS-PAGE were not heated (heating is known to dissociate the pentamer), and this is inconsistent with the results of Kim et al. (30) and Choi et al. (31). The reason for lack of phosphorylated PLB in control samples is unknown at this time. Consistent with previous studies (30,31), we also found that diabetes increases expression of monomeric unphosphorylated PLB. Since expression of SERCA2a decreases with diabetes, the ratio of SERCA2a to PLB decreases further, resulting in loss of SERCA2a activity. In this study, we also found that diabetes increases the amount of steady-state levels of phosphorylated PLB. Two distinct phosphorylated PLB bands were observed in 8D samples, likely reflecting the mono- and diphosphorylated forms of PLB. At this time, we are

uncertain as to which amino residue (serine-16 or threonine-17) is phosphorylated in the monophosphorylated form. These data are also inconsistent with those of Choi et al. (31), who found that diabetes decreases the amount of serine-16 and threonine-17 phosphorylation of PLB. The reason(s) for this discrepancy is not known at this time. We also found that insulin treatment significantly reduces steady-state levels of diphosphorylated PLB, but did not decrease the amount of monophosphorylated PLB.

In conclusion, data from the present study suggest that in addition to a decreases in expression SERCA2a, an increase in PLB and concomitant decreases in SERCA2a-to-PLB ratio, prolongation of cardiac relaxation rate may also be attributed to diabetes-induced increase in formation AGEs (crosslinking as well as noncrosslinking) on SERCA2a. Our data also show 2 weeks of insulin treatment initiated after 6 weeks of diabetes significantly improved cardiac function and also prevented formation of crosslinking AGEs on SERCA2a. In future studies, we intend to treat animals with aminoguanidine (blocker of AGEs) to establish a cause-effect relationship.

ACKNOWLEDGMENTS

This work was supported in part by grants from the National Institutes of Health (HL66898) and the Ralph W. and Grace R. Showalter Foundation.

Mass spectrometry was done at Indiana University School of Medicine, Proteomics Core Facility with support from the Indiana Genomic Initiative (INGEN).

The authors thank Sarah Ingersoll for technical assistance.

REFERENCES

1. Rubler S, Dlugash J, Yuceoglu YZ, Kumral T, Branwood AW, Grishman A: New type of cardiomyopathy associated with diabetic glomerulo-sclerosis. *Am J Cardiol* 30:595–560, 1972
2. Hamby RI, Zoneraich S, Sherman S: Diabetic cardiomyopathy. *JAMA* 229:1749–1754, 1974
3. Asmal AC, Leary WP, Thandroyen FS: Diabetic heart disease. *Afr Med J* 57:788–790, 1980
4. Reagan TJ, Lyons MM, Ahmed SS, Levinson GE, Oldewurtel HA, Ahmad MR, Haider B: Evidence for cardiomyopathy in familiar diabetes mellitus. *J Clin Invest* 60:885–899, 1977
5. Fein FS: Diabetic cardiomyopathy. *Diabetes Care* 13 (Suppl. 4):S1169–S1179, 1990
6. Bell DS: Diabetic cardiomyopathy: a unique entity or a complication of coronary artery disease. *Diabetes Care* 18:708–714, 1995
7. Regan TJ: Congestive heart failure in the diabetic. *Annu Rev Med* 34:161–168, 1983
8. Chatham JC, Forder JR, McNeill JH (Eds.): *The Diabetic Heart*. Boston, MA, Kluwer Academic Press, 1996
9. Tahiliani AG, McNeill JH: Diabetes-induced abnormalities in the myocardium. *Life Sci* 38:959–974, 1986
10. Dhalla NS, Lui X, Panagia V Takeda N: Subcellular remodeling and heart dysfunction in chronic diabetes. *J Cardiovasc Res* 40:239–247, 1998
11. Way KJ, Katai N, King GL: Protein kinase C and the development of diabetic vascular complications. *Diabet Med* 18:945–959, 2001
12. Sweadner KJ, Donnet C: Structural similarities of Na, K-ATPase and SERCA, the Ca(2+)-ATPase of the sarcoplasmic reticulum. *Biochem J* 356:685–704, 2001
13. Lee AG, East JM: What the structure of a calcium pump tells us about its mechanism. *Biochem J* 356:665–683, 2001
14. MacLennan DH, Rice WJ, Green NM: The mechanism of Ca2+ transport by sarco(endo)plasmic reticulum Ca2+-ATPases. *J Biol Chem* 272:28815–28818, 1997
15. MacLennan DH, Brandl CJ, Korczak B, Green NM: Amino-acid sequence of a Ca^{2+} + Mg^{2+}-dependent ATPase from rabbit muscle sarcoplasmic reticulum, deduced from its complementary DNA sequence. *Nature* 316: 696–700, 1985
16. MacLennan DH, Green NM: Pumping ions. *Nature* 405:633–634, 2000
17. Toyoshima C, Nomura H: Structural changes in the calcium pump accompanying the dissociation of calcium. *Nature* 418:605–611, 2002
18. Toyoshima C, Nakasako M, Nomura H, Ogawa H: Crystal structure of the calcium pump of sarcoplasmic reticulum at 2.6 A resolution. *Nature* 405:647–655, 2000
19. Toyoshima C, Nomura H, Sugita Y: Crystal structures of Ca2+-ATPase in various physiological states. *Ann N Y Acad Sci* 986:1–8, 2003
20. MacLennan DH, Kimura Y, Toyofuku T: Sites of regulatory interaction between calcium ATPases and phospholamban. *Ann N Y Acad Sci* 853:31–42, 1998
21. Simmerman HK, Jones LR: Phospholamban: protein structure, mechanism of action, and role in cardiac function. *Physiol Rev* 78:921–947, 1998
22. Toyoshima C, Asahi M, Sugita Y, Khanna R, Tsuda T, MacLennan DH: Modeling of the inhibitory interaction of phospholamban with the Ca2+ ATPase. *Proc Natl Acad Sci USA*. 100:467–472, 2003
23. Penpargkul S, Fein F, Sonnenblick EH, Scheuer J: Depressed cardiac sarcoplasmic reticular function from diabetic rats. *J Mol Cell Cardiol* 13:303–309, 1981
24. Ganguly PK, Pierce GN, Dhalla KS, Dhalla NS: Defective sarcoplasmic reticular calcium transport in diabetic cardiomyopathy. *Am J Physiol* 244:E528–E535, 1983
25. Lopaschuk GD, Tahiliani AG, Vadlamudi RV, Katz S, McNeill JH: Cardiac sarcoplasmic reticulum function in insulin- or carnitine-treated diabetic rats. *Am J Physiol* 245:H969–H976, 1983
26. Teshima Y, Takahashi N, Saikawa T, Hara M, Yasunaga S, Hidaka S, Sakata T: Diminished expression of sarcoplasmic reticulum Ca(2+)-ATPase and ryanodine sensitive Ca(2+)channel mRNA in streptozotocin-induced diabetic rat heart. *J Mol Cell Cardiol* 32:655–664, 2000
27. Zhong Y, Ahmed S, Grupp IL, Matlib MA: Altered SR protein expression associated with contractile dysfunction in diabetic rat hearts. *Am J Physiol* 281:H1137–H1147, 2001
28. Netticadan T, Temsah RM, Kent A, Elimban V, Dhalla NS: Depressed levels of Ca^{2+}-cycling proteins may underlie sarcoplasmic reticulum dysfunction in the diabetic heart. *Diabetes* 50:2133–2138, 2001
29. Razeghi P, Young ME, Cockrill TC, Frazier OH, Taegtmeyer H: Downregulation of myocardial myocyte enhancer factor 2C and myocyte enhancer factor 2C-regulated gene expression in diabetic patients with nonischemic heart failure. *Circulation* 106:407–411, 2002
30. Choi KM, Zhong Y, Hoit BD, Grupp IL, Hahn H, Dilly KW, Guatimosim S, Lederer WJ, Matlib MA: Defective intracellular Ca(2+) signaling contributes to cardiomyopathy in type 1 diabetic rats. *Am J Physiol Heart Circ Physiol* 283:H1398–H1408, 2002
31. Kim HW, Ch YS, Lee HR, Park SY, Kim YH: Diabetic alterations in cardiac sarcoplasmic reticulum Ca2+-ATPase and phospholamban protein expression. *Life Sci* 70:367–379, 2001
32. Norby FL, Wold LE, Duan J, Hintz KK, Ren J: IGF-I attenuates diabetes-induced cardiac contractile dysfunction in ventricular myocytes. *Am J Physiol Endocrinol Metab* 283:E658–666, 2002
33. Trost SU, Belke DD, Bluhm WF, Meyer M, Swanson E, Dillmann WH: Overexpression of the sarcoplasmic reticulum Ca^{2+}-ATPase improves myocardial contractility in diabetic cardiomyopathy. *Diabetes* 51:1166–1171, 2002
34. Vetter R, Rehfeld U, Reissfelder C, Weiss W, Wagner KD, Gunther J, Hammes A, Tschope C, Dillmann W, Paul M: Transgenic overexpression of the sarcoplasmic reticulum Ca2+ATPase improves reticular Ca2+ handling in normal and diabetic rat hearts. *FASEB J* 16:1657–1659, 2002
35. Russ M, Reinauer H, Eckel J: Diabetes-induced decrease in the mRNA coding for sarcoplasmic reticulum Ca(2+)-ATPase in adult rat cardiomyocytes. *Biochem Biophys Res Commun* 178:906–912, 1991
36. Zarain-Herzberg A, Yano K, Elimban V, Dhalla NS: Cardiac sarcoplasmic reticulum Ca(2+)-ATPase expression in streptozotocin-induced diabetic rat heart. *Biochem Biophys Res Commun* 203:113–120, 1994
37. Ye G, Metreveli NS, Ren J, Epstein PN: Metallothionein prevents diabetes-induced deficits in cardiomyocytes by inhibiting reactive oxygen species production. *Diabetes* 52:777–783, 2003
38. Candido R, Forbes JM, Thomas MC, Thallas V, Dean RG, Burns WC, Tikellis C, Ritchie RH, Twigg SM, Cooper ME, Burrell LM: A breaker of advanced glycation end products attenuates diabetes-induced myocardial structural changes. *Circ Res* 92:785–792, 2003
39. Ferrington DA, Krainev AG, Bigelow DJ: Altered turnover of calcium regulatory proteins of the sarcoplasmic reticulum in aged skeletal muscle. *J Biol Chem* 273:5885–5891, 1998
40. Bidasee KR, Dincer UD, Besch HR Jr: Ryanodine receptor dysfunction in hearts of streptozotocin-induced diabetic rats. *Mol Pharmacol* 60:1356–1364, 2001
41. Bidasee KR, Nallani K, Besch HR Jr, Dincer UD: Streptozotocin-induced

diabetes increase disulfide bond formation on cardiac ryanodine receptor (RyR2). *J Pharmacol Expt Ther* 5:989–998, 2003
42. Bidasee KR, Nallani K, Yu Y, Cocklin RR, Zhang Y, Wang M. Dincer UD, Besch HR Jr: Chronic diabetes increases advanced glycation end products on cardiac ryanodine receptors (RyR2). *Diabetes* 52:1825–1836, 2003
43. Dincer UD, Bidasee KR, Guner S, Tay A, Ozcelikay AT, Altan VM: The effect of diabetes on expression of β_1-, β_2-, and β_3-adrenoreceptors in rat hearts. *Diabetes* 50:455–461, 2001
44. Zhang K, Li YF, Patel KP: Blunted nitric oxide-mediated inhibition of renal nerve discharge within PVN of rats with heart failure. *Am J Physiol Heart Circ Physiol* 281:H995–H1004, 2001
45. Bidasee KR, Nallani K, Henry B, Dincer UD, Besch HR Jr: Chronic diabetes alters function and expression of ryanodine receptor calcium-release channels in rat hearts. *Mol Cell Biochem* 249:113–123, 2003
46. Cocklin RR, Zhang Y, O'Neill KD, Chen NX, Moe SM, Bidasee KR, Wang M: Identity and localization of advanced glycation end products on human beta(2)-microglobulin using matrix-assisted laser desorption/ionization time-of-flight mass spectrometry. *Anal Biochem* 314:322–325, 2003
47. Zhang Y, Cocklin RR, Bidasee KR, Wang M: Rapid determination of advanced-glycation end products of proteins using MALDI-TOF mass spectrometry and PERL script peptide searching algorithm. *J Biomol Tech* 14:224–230, 2003
48. Dincer UD, Onay A, Ari N, Ozcelikay AT, Altan VM: The effects of diabetes on β-adrenoceptor mediated responsiveness of human and rat atria. *Diabetes Res Clin Pract* 40:113–122, 1998
49. Afzal N, Ganguly PK, Dhalla KS, Pierce GN, Singal PK, Dhalla NS: Beneficial effects of verapamil in diabetic cardiomyopathy. *Diabetes* 37:936–942, 1988